

# CONTROL STRATEGY OF A 6 MVA SERIES CONNECTED SYNCHRONOUS GENERATOR FOR WIND POWER

*Dr. Mona F. Moussa\**, *Prof. Yasser G. Dessouky\*\**, *Prof. Barry W. Williams†*

*Arab Academy for Science and Technology and Maritime Transport, Miami, P.O. Box: 1029, Alexandria, EGYPT\**, *\*\**  
*Email\*: mona.moussa@yahoo.com*

*Faculty of Engineering, Strathclyde University, Glasgow, U.K.†*

**Keywords:** Induction machine, synchronous generator, grid connection, wind energy conversion, maximum power tracking.

## Abstract

A new proposal for a wind power system utilizes a variable-speed generator, since it has a higher energy capturing and converting efficiency than a fixed-speed system. This paper describes a vector control strategy for a direct-driven Series Connected Synchronous Generator SCSG, which is connected to the power network through a controlled three phase rectifier and a PWM inverter. The generator side converter is controlled to obtain maximum power from the incident wind and the grid-side inverter maintains a constant DC-link voltage. Simulated results are given to illustrate the performance of the system.

## 1 Introduction

Renewable energy systems require no source of fossil or nuclear fuel and their environment impact is deemed low [1]. Green electricity generation through renewable energy sources for sustainable development and environment protection is a major challenge to the modern world. Over the last ten years, global wind energy capacity has increased rapidly and is the fastest developing renewable energy technology. Early technology used in wind turbines was based on squirrel-cage induction generators directly connected to the grid. Recently, the technology has developed towards variable speed. Power electronics plays an important role in wind power systems where converters are used to match the characteristics of wind turbines with the requirements of grid connection, including frequency, voltage, control of active and reactive power and harmonics [2]. The common way to convert the low-speed, high-torque mechanical power to electrical power uses a step-up gearbox and a standard speed generator. The gearbox adapts the low speed of the turbine rotor to the high speed of the generator [2]. The SCSG is an induction machine- in construction- therefore a gear box is required. In modern variable speed wind turbines, a maximum power tracker adjusts the rotational speed to maximize turbine power output [3-7].

The Series Connected Synchronous Generator (SCSG) was proposed to produce sinusoidal output voltage with a frequency dependent only on speed. SCSG is a slip ring induction machine

whose stator and rotor windings are connected in series with a sequence of two phases reversed as shown in Fig. 1. As a result, stator and rotor MMFs will rotate at the same speed ( $\omega_c$ ) but in opposite directions. The self-excitation process commences as with the self-excited induction generator using excitation capacitors. With reference to Fig. 2, electro-mechanical energy conversion is possible only when stator and rotor MMFs rotate synchronously at an absolute speed ( $\omega_c$ ) equal to half rotor speed ( $\omega$ ). The SCSG has been analyzed using Floquet theory for solving the resulting differential equations with time varying coefficients [8]-[9]. Another approach was presented in [10] to examine the effects of these parameters based on a deduced phase diagram.

However reactive power management is a major concern, not only to compensate for the reactive power requirements of the wind farm itself but also to support the system voltage, particularly wind farms based on fixed speed SCSG. The capacitive self-excitation is possibly the cheapest and simplest technique to implement a SCSG. However, it must be considered that some additional mechanism for magnetizing the machine should be included in the design to avoid the possibility that all residual magnetism is lost. To improve SCSG operation different techniques have been proposed, using different types of excitation: active and passive. Similar to the conventional induction generator some of these techniques use inverters to feed the SCSG reactive power and field-oriented controllers. This gives better efficiency and voltage regulation. While most of the current turbines are connected to the medium-voltage system, large offshore wind farms may be connected to high-voltage and ultra high-voltage systems. The transformer is normally located close to the wind turbines to avoid high current flowing in long low-voltage cables [2].

This paper explores a direct drive SCSG system for a wind turbine. The machine side three phase converter maintains the DC-link voltage constant. In contrast, the grid-side three phase converter, which uses a vector control strategy, operates as a driver controlling the generator operating at optimum rotor speed to obtain maximum energy from the wind, feeds generated energy into the grid and adjusts the amount of the active and reactive power delivered to the grid. It also decreases the current total-harmonic-distortion (THD) injected into the grid. Both the DC-link voltage and dq currents of grid side are controlled by PI controllers. The control algorithm uses stator-flux oriented control, with the d-axis aligned to the stator flux axis and the q-axis aligned

close to the stator voltage axis. A field-oriented scheme enables the control of two independent variables:  $i_q$  or stator torque current and  $i_d$  or stator field current.

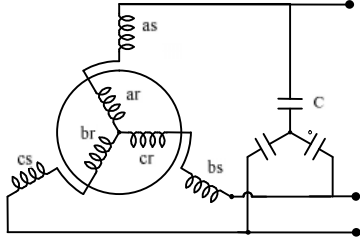


Fig 1: Schematic diagram for SCSG.

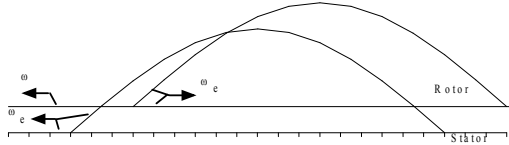


Fig 2: MMF for stator and rotor in SCSG.

## 2 D-Q model representation of the SCSG

To analyze this generator, a reference frame that rotates synchronously with stator and rotor MMFs was chosen. Since the rotor actually rotates at double the reference frame speed, and with reference to Fig. 3, the following relation holds for all rotor positions.

$$\theta = \beta \quad (1)$$

Reversing stator and rotor phase sequence windings can be expressed by:

$$(i_{ar} = i_{as}), (i_{br} = i_{cs}), (i_{cr} = i_{bs}) \quad (2)$$

Equivalent stator and rotor d-q currents in terms of actual phase currents and mutual displacements are given by the transformations [11].

$$\begin{bmatrix} i_{dr} \\ i_{qr} \end{bmatrix} = \frac{2}{3} \begin{bmatrix} \cos(\beta) & \cos\left(\beta + \frac{2\pi}{3}\right) & \cos\left(\beta - \frac{2\pi}{3}\right) \\ -\sin(\beta) & -\sin\left(\beta + \frac{2\pi}{3}\right) & -\sin\left(\beta - \frac{2\pi}{3}\right) \end{bmatrix} \begin{bmatrix} i_{ar} \\ i_{br} \\ i_{cr} \end{bmatrix} \quad (3)$$

$$\begin{bmatrix} i_{ds} \\ i_{qs} \end{bmatrix} = \frac{2}{3} \begin{bmatrix} \cos(\theta) & \cos\left(\theta - \frac{2\pi}{3}\right) & \cos\left(\theta + \frac{2\pi}{3}\right) \\ \sin(\theta) & \sin\left(\theta - \frac{2\pi}{3}\right) & \sin\left(\theta + \frac{2\pi}{3}\right) \end{bmatrix} \begin{bmatrix} i_{as} \\ i_{bs} \\ i_{cs} \end{bmatrix} \quad (4)$$

Fig 3: Axes of 3-phase symmetrical induction motor.

Fig 4: Basic d-q circuit model of SCSG.

Substituting (1) and (2) into (3) and comparing the result with (4) yields:

$$\begin{cases} i_{ds} = i_{dr} = i_d \\ i_{qs} = -i_{qr} = i_q \end{cases} \quad (5)$$

Implementing the conditions derived in (5) into the d-q model results in the interconnections between axes equivalent coils shown in Fig. 3. It is seen that:

$$\begin{cases} v_d = v_{ds} + v_{dr} \\ v_q = v_{qs} - v_{qr} \end{cases} \quad (6)$$

The relation between d-q axes voltages and currents can be expressed as:

$$\begin{bmatrix} v_d \\ v_q \end{bmatrix} = \begin{bmatrix} R + L_d P & -L_q \omega_e \\ L_d \omega_e & R + L_q P \end{bmatrix} \begin{bmatrix} i_d \\ i_q \end{bmatrix} \quad (7)$$

$$\text{where, } R = R_s + R_r, L_d = L_s + L_r + 2M,$$

$$L_q = L_s + L_r - 2M \quad (8)$$

$L_s, L_r$ : stator and rotor self inductances,  $L_d, L_q$ : self inductances of (d) and (q) axes,  $M$ : maximum mutual inductance between rotor and stator, and  $R_s, R_r$ : stator and rotor resistance.

The series connection between stator and rotor phase windings results in effective saliency as indicated by the difference in axes inductances which implies synchronous operation of this machine.

To take saturation in the iron parts into account,  $L_d$  and  $L_q$  are represented as a function of  $i_d$  and  $i_q$  as follows. The peak magnetization current,  $i_m$  is related to d-q currents by:

$$i_m = \sqrt{(i_{ds} + Ki_{dr})^2 + (i_{qs} + Ki_{qr})^2} \quad (9)$$

Substituting by (5) into (9) yields:

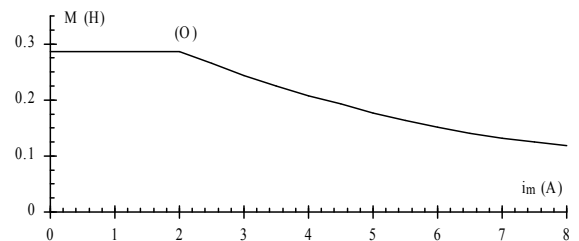


Fig 5: Mutual inductance & magnetization current relationship.

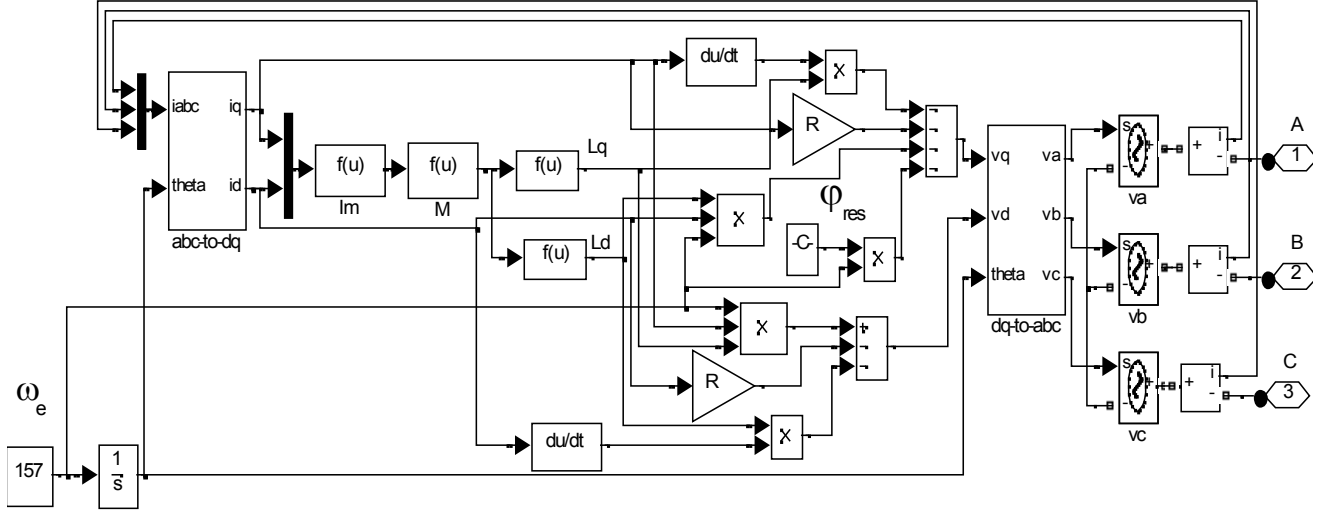


Fig 6: SIMULINK block diagram of SCSG.

$$i_m = \sqrt{(1+K)^2 i_d^2 + (1-K)^2 i_q^2} \quad (10)$$

From an open circuit test, the relationship between the RMS air gap voltage  $V_g$  and magnetization current  $I_\mu$  is evaluated. For each point,  $M$  and  $i_m$  are calculated as:

$$M = V_g / \omega I_\mu \quad \text{and} \quad i_m = \sqrt{2} I_\mu$$

The relationship between  $M$  and  $i_m$  shown in Fig. 5 can be expressed mathematically by a polynomial. Self inductances are related to leakage and mutual inductances by:

$$L_s = l_s + KM, \quad L_r = l_r + KM \quad (11)$$

### 3 Simulink model using Matlab

A model of the series connected synchronous generator has been proposed using MATLAB SIMULINK as shown in Fig. 6. Voltage build up occurs because of the residual magnetism  $\Phi_{res}$  which appears in the q-axis component of the voltage. The machine is connected to a fixed permanent capacitor for excitation and the model is tested at no load.

### 4 System control

In the variable-speed generation system, the wind turbine can be operated at the maximum power operating point for various wind speeds by adjusting the shaft speed optimally to achieve maximum power point tracking (MPPT) control to maximize wind power capture [12-13]. The rating of the wind power converter is 6 MVA apparent power, targeting a 5 MW wind turbine. A simplified scheme of the proposed wind power system is shown in Fig. 7. The grid connection to a typical wind farm interconnection voltage level of 10 kV requires a medium voltage transformer. The system is controlled by a field oriented control (FOC) technique. The generator side converter is a three phase controlled rectifier functioning to keep the DC-link voltage constant regardless of the magnitude of the machine-side power. On the grid-side, a vector-control approach is used, with a reference frame oriented along the supply voltage vector, enabling

independent control of the active and reactive power flowing to the supply. The PWM converter is current regulated.

The active and reactive power control is achieved by controlling direct and quadrature current components, respectively through two channel control loops. As to active power channel, the MPPT control circuit generates the d-axis current reference for active power control. This assures that all the power from the rectifier is instantaneously transferred to the grid by the inverter. The second channel controls the reactive power by setting a q-axis current reference to a current control loop, where the  $i_q$  demand determines the displacement factor on the supply-side of the inductors. The q-axis component of current equals zero in order to reduce the compensation of the generator reactive power since it takes the reactive power from the constant capacitance in contrast to the synchronous generator which feeds the reactive power in addition to the active power [14-17]. A step-up transformer is used on the grid side. However the step-up transformer is usually located at ground level. There are cost considerations for the architecture of the generator and converter architecture as described in [15].

The PLL technique is used to extract the phase angle of the grid voltages [18-20]. The PLL is implemented in the dq synchronous reference frame, and its schematic is illustrated in Fig. 8. This structure needs the coordinate transformation from abc to dq, and the lock is realized by setting the reference  $U_d^*$  to zero. A regulator, usually PI, is used to control this variable, and the output of this regulator is the grid frequency. After integration of the grid frequency, the utility voltage angle is obtained, which is fed back to the  $\alpha\beta$  to dq transformation module to transform into the synchronous rotating reference frame. This algorithm has better rejection of grid harmonics, notches, and other kinds of disturbances [21-23].

The grid-connected inverter generates a PWM voltage with a fundamental component at the grid frequency, and is also able to supply the active nominal power to the grid.

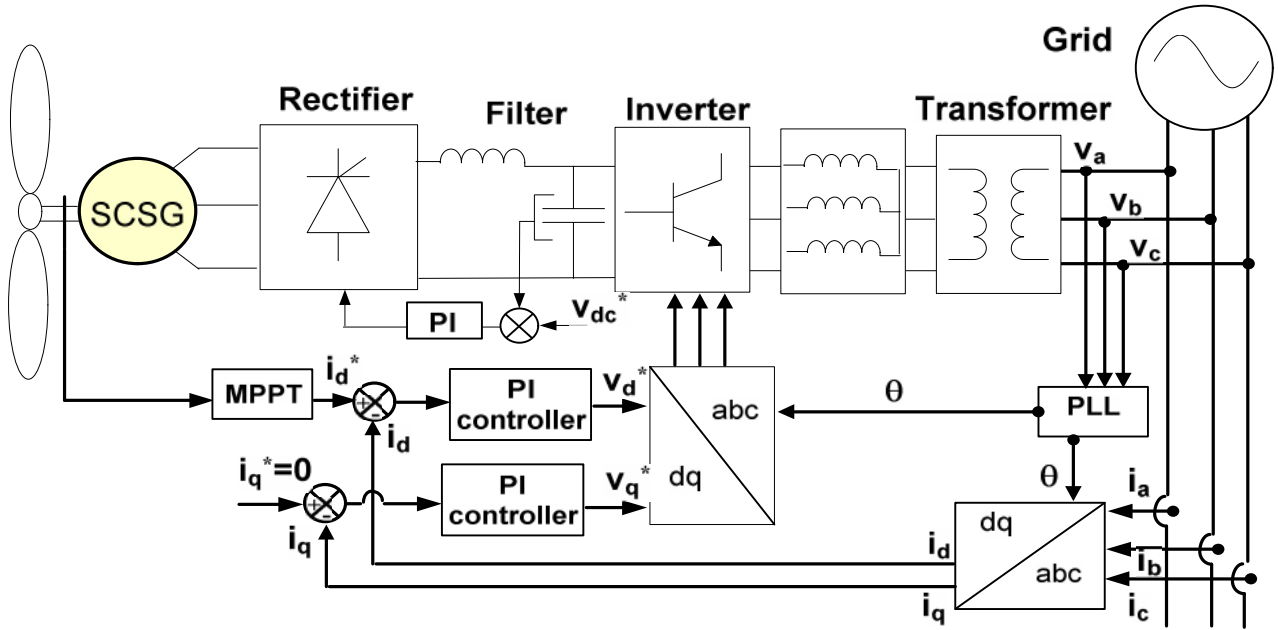


Fig. 7: Diagram of the proposed 6MVA wind power system.

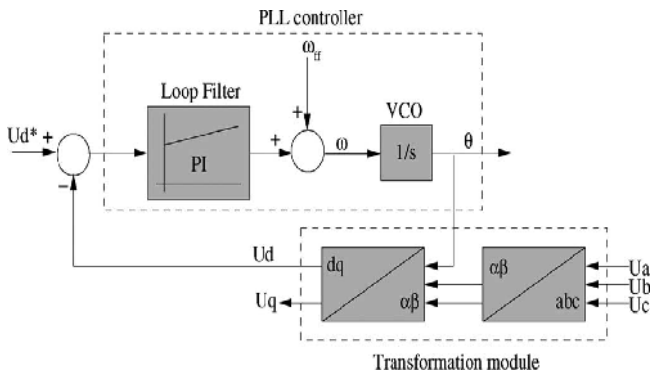
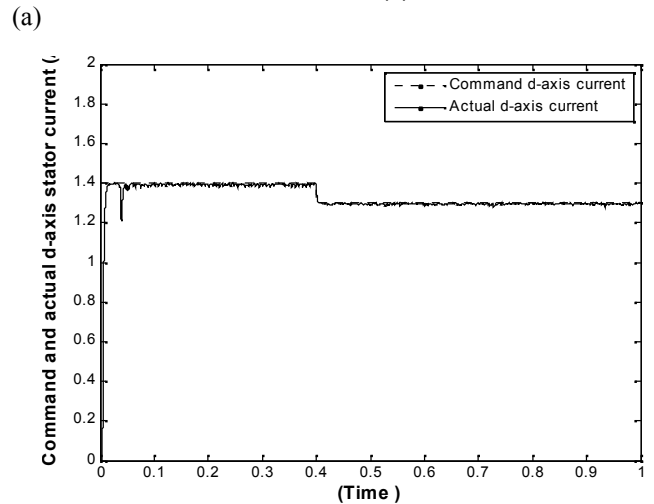
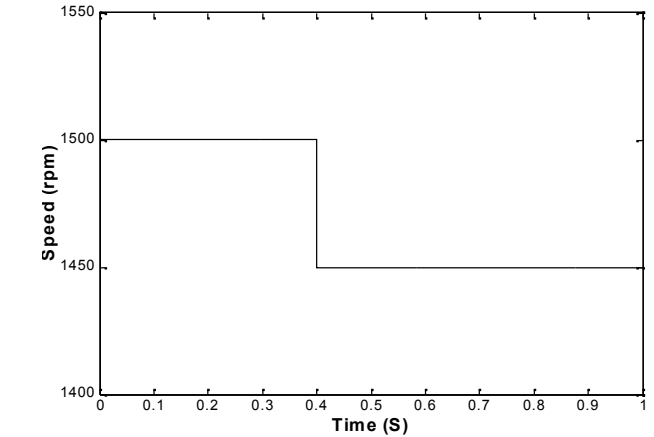


Fig 8: General structure of the three-phase  $dq$  PLL method.

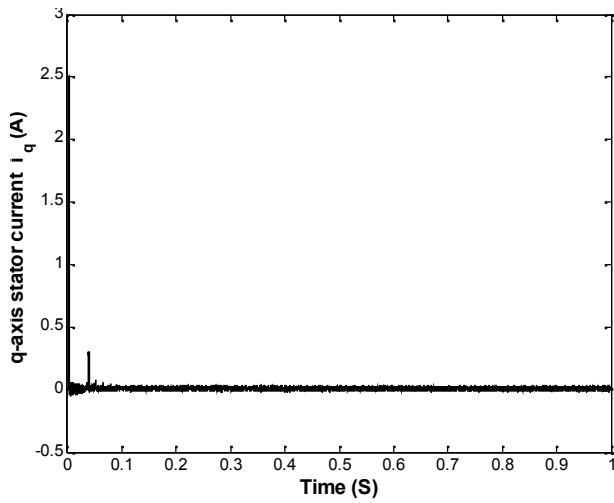
## 5 Results

The system is proposed for 6MVA wind power generation. However, the prototype a scaled down 6kVA rated system. The line generation voltage is 690V. A permanent capacitor (300 $\mu$ F), which supports the self excitation for the SCSG and also provides the reactive power requirements of the inductive elements connected between the generator and the grid. This results in a no load voltage of almost 690V and allows for a load current corresponding to 6kVA before self excitation is lost. The wind turbine is connected to the SCSG through a gear box where the nominal shaft speed is 1500 rpm corresponding to 25Hz for the SCSG. The generator voltage is converted to dc where a feedback signal is used to regulate the dc link voltage at a constant value of 600V. A CSI inverter is used to convert the dc voltage into three-phase which is connected to the 11kV grid through a step up transformer. The inverter is controlled using a FOC technique. Simulation tests have been carried out in order to evaluate the adequacy and confirm the validity of the FOC system performance. A 3% step up change is applied to the speed command at time 4s. As a result, the MPPT circuit updates the command d-axis stator current  $i_d$  and the FOC will

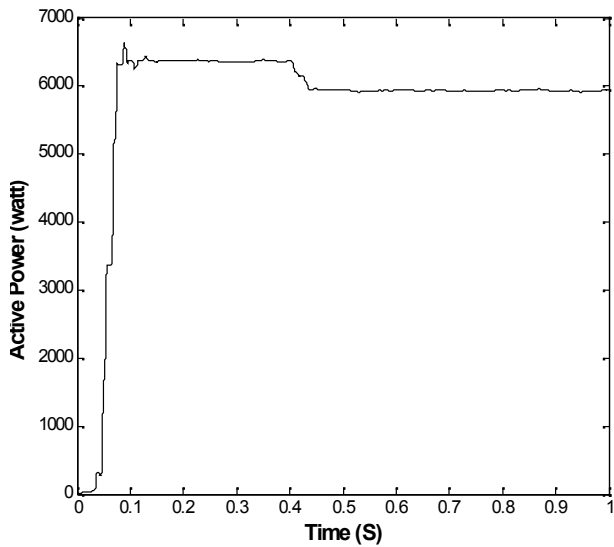
regulate the current to match the new value. Fig. 9 shows the behavior of the FOC system due to a 3% step change in the speed command.



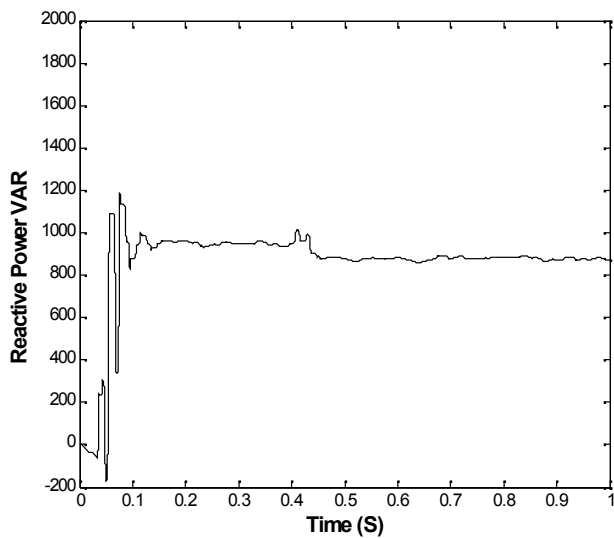
(b)



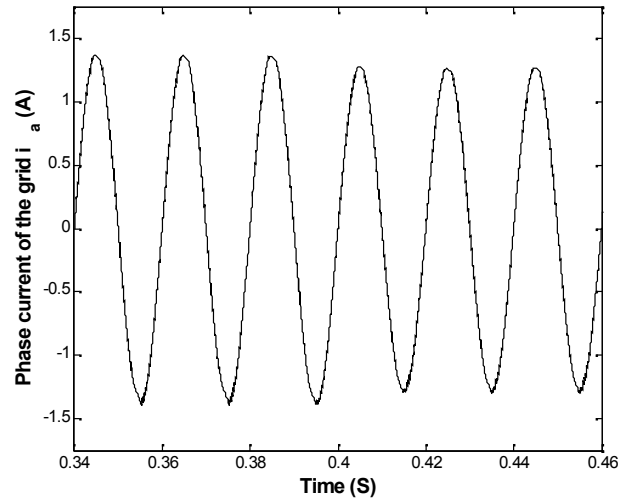
(c)



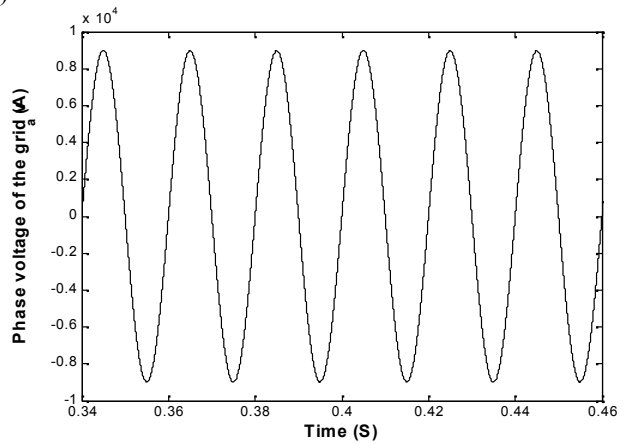
(d)



(e)



(f)



(g)

Fig 9: Simulink results of: (a) 3% step speed change, (b) grid d-axis current, (c) grid q-axis current, (d) active power supplied by SGSG, (e) reactive power from excitation capacitor to the grid, (f) grid phase current, and (g) grid phase voltage.

## 6 Conclusion

This paper discussed the control of a series connected synchronous generator for wind power application. Generalized machine theory was applied to the SCSG and a d-q model was presented. The model introduced machine, saturation and load representations. Self-excitation voltage build up was introduced. A vector-control technique was applied to the grid-side converter to realize optimal speed tracking and the active and reactive power independent regulation. The fundamental operational advantages have been verified and the SIMULINK results confirm that the vector control algorithm operates efficiently in the close loop control system to control active and reactive power independently. With assumptions for initial conditions, calculated results validate the model for transient state analysis. Finally, an overview of grid synchronization algorithms was given. Additionally, the system is capability of MPPT, harmonics elimination and load balancing.

## References

- [1] G. Martin, "Renewable energy gets the "green" light in Chicago, Power and Energy Magazine, vol. 1, no.1, pp. 34-39, Nov.-Dec. 2003.
- [2] Zhe Chen, Josep M. Guerrero, and Frede Blaabjerg, "A Review of the State of the Art of Power Electronics for Wind turbines," *IEEE Trans. on Power Electronics*, vol. 24, no. 8, pp. 1859-1875, August 2009.
- [3] A. K. Jain and V. T. Ranganathan, "Wound rotor induction generator with sensorless control and integrated active filter for feeding nonlinear loads in a stand-alone grid," *IEEE Trans. Ind. Electron.*, vol. 55, no. 1, pp. 218-228, Jan. 2008.
- [4] Maxime R. Dobuis, "Review of electromechanical conversion in wind turbines," *Electrical Power Processing. Nederland*, 2000, pp.70-73.
- [5] Pena R. Clare J C. Asher G M, "Doubly-fed induction generator using back-to-back PWM converters and its application to variable-speed wind energy generation," *IEE Proc. Elect. Power Appl*, 143(3), pp. 231-241.
- [6] Rabelo, B. Hofmann, W., "Control of an optimized power flow in wind power plants with doubly-fed induction generators," *Power Electronics Specialist Conference*, 2003, pp.1563-1568.
- [7] Huang Keyuan He Yikang, "Investigation of a matrix converter-excited brushless doubly-fed machine wind-power generation system," *The Fifth International Conference on Power Electronics and Drive Systems*, 2003, pp.743-748.
- [8] A.S. Mostafa, A.L. Mohamadein and E.M. Rashad, "Analysis of series connected wound rotor self excited induction generator," *IEE Proc. B*, Vol. 140, No. 5, Sept 1993.
- [9] A.S. Mostafa, A.L. Mohamadein and E.M. Rashad, "Application of Floquet's theory to the analysis of series-connected wound-rotor self-excited synchronous generator," *IEEE Trans. on EC*, Vol. 8, No. 3, Sept. 1993.
- [10] A.L. Mohamadein and E.A Shehata, "Theory and performance of series connected self excited synchronous generator," *IEEE Trans. on EC*, Vol. 10, No. 3, Sept. 1995.
- [11] E. Rashad, M. Abdel-Karim and Y.G. Dessouky, "Theory and analysis of three phase series connected parametric motors", *IEEE Trans. on EC*, Vol. 11, No. 4, Dec. 1996.
- [12] A. Faulstich, J. Steinke, F. Wittwer, "Medium Voltage Converter for Permanent Magnet Wind Power Generators up to 5 MW," *European Conference on Power Electronics*, 11-14 Sept, 2005.
- [13] M. Winkelkemper, F. Wildner, P. Steimer "6 MVA Five-Level Hybrid Converter for Wind power", *Conv. Proc., PESC*, Rhodes, Greece, 2008.
- [14] Keyuan Huang, Shoudao Huang, Feng She, Baimin Luo, and Luoqiang Cai, "A Control Strategy for Direct-drive Permanent-magnet Wind-power Generator Using Back-to-back PWM Converter", *International Conference on Electrical Machines and Systems, ICEMS 2008*, pp. 2283 – 2288.
- [15] H. Polinder, F. F. A. van der Pijl, G.-J. de Vilder, and P. J. Tavner, "Comparison of direct-drive and geared generator concepts for wind turbines," *IEEE Trans. Energy Conversion*, vol. 21, no. 3, pp. 725–733, Sep. 2006.
- [16] Markus Eichler, Philippe Maibach, Alexander Faulstich, "Full Size Voltage Converters for 5MW Offshore Wind Power Generators," *European Wind Energy Conference, EWEC'08*, 2008.
- [17] H. Ch. Chen, Ch. Wu, Ch. Chang, Y. Chang, and H. Lin, "Integral sliding-mode flux observer for sensorless vector-controlled induction motors," *System Science & Engineering (ICSSE) Conf.*, pp. 298-303, Aug. 2010.
- [18] S.-K. Chung, "A phase tracking system for three phase utility interface inverters," *IEEE Trans. Power Electron.*, vol. 15, no. 3, pp. 431–438, May 2000.
- [19] L. N. Arruda, S. M. Silva, and B. Filho, "PLL structures for utility connected systems," in *Proc. IEEE-IAS Annu. Meeting*, 2001, vol. 4, pp. 2655–2660.
- [20] S.-K. Chung, "Phase-locked loop for grid-connected three-phase power conversion systems," *Proc. Inst. Electr. Eng.-Electron. Power Appl.*, vol. 147, no. 3, pp. 213–219, May 2000.
- [21] P. Rodriguez, J. Pou, J. Bergas, I. Candela, R. Burgos, and D. Boroyevich, "Double synchronous reference frame PLL for power converters," in *Proc. IEEE PESC*, 2005, pp. 1415–1421.
- [22] M. C. Benhabib and S. Saadate, "A new robust experimentally validated phase-locked loop for power electronic control," *EPE J.*, vol. 15, no. 3, pp. 36–48, Aug. 2005.
- [23] S. Lee, J. Kang, and S. Sul, "A new phase detection method for power conversion systems considering distorted conditions in power system," in *Proc. IEEE-IAS Annu. Meeting*, 1999, vol. 4, pp. 2167–2172.